FINITE ELEMENT ANALYSIS APPLIED TO EVALUATION OF EFFECTIVE MATERIAL COEFFICIENTS FOR PIEZOELECTRIC FIBER COMPOSITES

Mariano Eduardo Moreno, 01mmoreno@gmail.com
Volnei Tita, voltita@sc.usp.br
Flávio Donizeti Marques, fmarques@sc.usp.br
University of São Paulo, Aeroelasticity Laboratory and Aeronautical Structures Group.
Av. Trabalhador São-carlense, 400, 13566-590, São Carlos, SP, Brazil

Abstract. *Piezoelectric fiber composites have several potential applications in aerospace industry due the high level design requirements that can be provided for this kind of material in applications such as structure health monitoring, precision positioning and vibration control or suppression. Difficulties in fiber manufacturing techniques and behavior prediction are the main obstacles to the practical implementation of this technology. In this work one procedure for determining effective properties of one ply made of unidirectional fibers from individual properties of the constituent materials and composite characteristics is presented and discussed. The procedure is based in the modeling of a Representative Volume Element (RVE) or a unit cell by finite element method. The RVE is analyzed under several loading and boundary conditions in order to evaluate of the effective material coefficients (elastic, dielectric end piezoelectric). The results are discussed and compared with analytical and numerical results presented by other researchers.*

Keywords*: piezoelectric fiber composites, finite element analysis, effective material properties*

1. INTRODUCTION

Active fiber composites have been largely studied during the last years applied as actuator and/or sensor in smart structures with large potential use in aerospace industry. Several approaches have been studied in order to describe the electromechanical behavior of the piezoelectric coupling in composite materials. These approaches are experimental, analytical, numerical or hybrid. Frequently, authors apply more than one approach to obtain a better evaluation of the material coefficients and electromechanical behavior.

Several researches like described by Chan and Unsworth (1989) as well as by Smith and Auld (1991) are based in analytical approaches that are limited in terms of loading cases in which they can be applied. Researches like described by Dunn and Taya (1993) employs micro-mechanical theory coupled to the electro-elastic solution study ellipsoidal inclusions into a infinite piezoelectric medium. Bisegna and Luciano (1996 and 1997) generalize the Hashin-Shtrikman principles in order to determine the limits of all piezoelectric properties of selected materials. Rodriguez-Ramos *et al.* (2001) and Bravo-Castillero *et al.* (2001) apply the asymptotic homogenization to composites (piezoelectric or not) with fibers in square arrangement. Guinovart-Díaz *et al.* (2001 and 2002) and Sevostianov (2001) also apply the asymptotic homogenization, but to models with hexagonal symmetry of fibers and random distribution, respectively, both with good agreement.

Finite element techniques using a representative volume element (unit cell) were employed by Gaudenzi (1997) to obtain the properties for piezo-composite patches applied on metallic plates. Poizat and Sester (1999) show how to obtain two effective piezoelectric coefficients (longitudinal and transverse). Petterman and Suresh (2000) use unit cell models applied to 1-3 piezo-composites. Paradies e Melnykowycz (2007) study the influence of interdigital electrodes over mechanical properties of PZT fibers.

Melnykowycz *et al.* (2006) characterize the performance of intelligent composite materials reinforced with fiberglass and integrated PZT fibers.

The research of Kar-Gupta and Venkatesh (2005, 2007a and 2007b) is about the influence of fiber distribution in 1-3 piezoelectric composites considering both, fiber and matrix, with piezoelectric properties. Analytical techniques discussed can not consider fiber distribution. Therefore, finite element analysis are presented and discussed. Berger *et al.* (2005) evaluate effective material properties of piezoelectric composites using analytical and numerical techniques.

Azzouz *et al.* (2001) improve the properties of MIN6 element (three nodes aniso-parametric element) to take into account the modeling of AFC (active fiber composite) and MFC ™ (macro fiber composite). Tan and Vu-Quoc (2005) present a solid-shell element formulation to model active composite structures considering large deformation and displacements. The element has displacement and electrical degrees of freedom. The authors ensure the efficiency and precision in the analysis of multilayer composite structures submitted to large deformation, including piezoelectric layers.

Panda and Ray (2006, 2008) include temperature dependence to the piezoelectric composite properties. The studied structure is a composite plate with piezoelectric composite patches.

Dent *et al.* (2005) identify positive and negative characteristics of PZF fibers for use in piezoelectric composites

through extensive evaluation of commercially available fibers due to their morphology, micro-structure and phase-composition.

Paik *et al.* (2007) employ direct numerical simulation – a simulation using detailed modeling, incorporating every micro-structure – justifying that unit cell models are limited to predict the behavior of piezoelectric fiber composites.

In this work one procedure for determining effective properties of one ply made of unidirectional fibers from individual properties of the constituent materials and composite characteristics is presented and discussed. The procedure is based on the modeling of a RVE (unit cell) by finite element method. The RVE is analyzed under several loading and boundary conditions in order to evaluate the effective material coefficients (elastic, dielectric end piezoelectric). All analysis were carried using the software ANSYS®. Two different fiber arrangement analysis are presented, square and hexagonal, and the advantages/disadvantages of each model are discussed. There are RVE chosen specifically for some analysis, in order to make possible the use of suitable boundary conditions to represent the periodicity of the unit cell.

2. BACKGROUND

2.1. Representative volume element

According to the fiber arrangement for periodic composites, a RVE can be chosen in such a way that with the appropriated boundary conditions it can represent the behavior of the whole composite. Figure 1(a) shows a composite with unidirectional fibers in hexagonal arrangement and fig. 1(b) shows the correspondent unit cell (RVE). The same idea can be used for other arrangements. For example to a square arrangement the unit cell is the fiber centered in a cubic portion of matrix as showed in fig. 2(a).

The fig. 2(a) also presents the designation given to the faces of RVE, adopted to help the explanation about loading and boundary conditions. According to its location, the faces of the RVE are designated as X+, X-, Y+, Y-, Z+ and Z-. In all analysis the fiber is continuous and orientated along the z-axis.

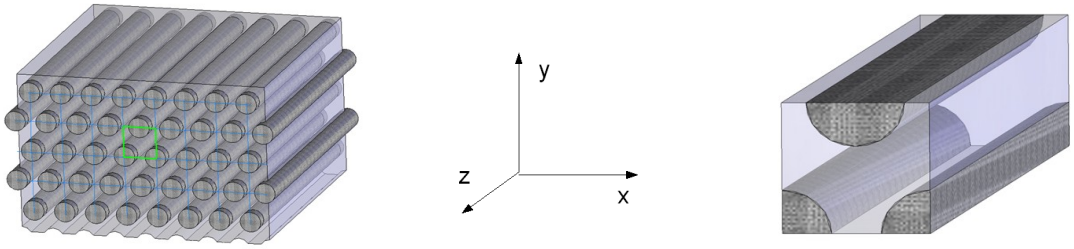

(a) (b)

Figure 1. (a) Composite with unidirectional fibers in hexagonal arrangement; (b) correspondent unit cell

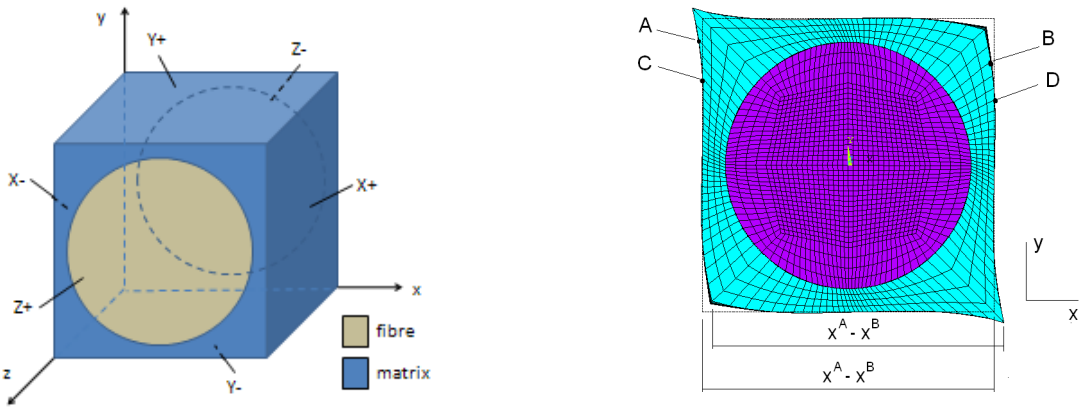

(a) (b)

Figure 2. (a) Square arrangement unit cell; (b) Correspondence between opposite sides

Considering two opposite point, A and B, as showed in fig. 2(b) and other set of opposite points, C and D, their displacements, u_i, respecting the periodicity of the RVE can be written in terms of the average unit cell strain (S_{ij}) as (Berger *et al.*, 2005):

$$u_i^A = u_i^B + \bar{S}_{ij}\left(x_j^A - x_j^B\right) \tag{1}$$

$$u_i^C = u_i^D + \bar{S}_{ij}\left(x_j^C - x_j^D\right) \tag{2}$$

The same relations are also valid to the electrical degrees of freedom. Subtracting both equations and having in mind that the average S_{ij} is the same in both equations and $x^A - x^B = x^C - x^D$ (as can be seen in fig. 2(b)), the constraint equation can be rewritten as following, respectively to displacement and electrical potential degrees of freedom.

$$u_i^A - u_i^C = u_i^B - u_i^D \tag{3}$$

$$\varphi^A - \varphi^C = \varphi^B - \varphi^D \tag{4}$$

. Where φ is the electrical potential correspondent to the node indicated by the superscript index. The last two equations represents a parallelism condition between the sides AC and BD. This condition must be applied for each pair of nodes in opposite sides of the unit cell (in vertical and horizontal directions) and must be repeated along the depth of the cell. In the analysis presented it is not necessary to specify these conditions for all the analyzed cases because sometimes the displacement and electrical boundary conditions already ensures this parallelism restriction. It is interesting to avoid the application of this conditions because there is a large number of equations that must be input. Automatic procedures to search opposite nodes and applying restrictions must be used. In the loading cases involving shear forces this procedure cannot be avoided, and the constraint equations has to be used in the sides submitted to the shear loading.

2.2. Piezoelectric composites

Piezoelectric composites are designated by two numbers representing how many dimensions are considered infinite length. The first number is referred to the fiber, for example, 1 (one) represents continuous fiber and 0 (zero) for chopped fiber. The second number refers to the matrix. If the matrix is considered of "infinite size" over all three coordinated directions it receives the number 3. In this work composites with continuous unidirectional fibers with a big number of plies (thick plates) are considered, or using the proper designation, 1-3 composites.

Piezoelectric problems are those one which an electrical potential gradient cause mechanical strains, as well as mechanical strains induces an electrical potential. The material properties (material coefficient matrix) for this case must include the dielectric coefficients and mechanical-electrical coupling coefficients (the piezoelectric coefficients), besides the usual mechanical parameters. Therefore, the constitutive equations which represent the complete electromechanical behavior can be described through the following system of equations, written in matrix notation:

$$\begin{Bmatrix} \{T\} \\ \{D\} \end{Bmatrix} = \begin{bmatrix} [C] & [e] \\ [e]^T & -[\varepsilon] \end{bmatrix} \begin{Bmatrix} \{S\} \\ -\{E\} \end{Bmatrix} \tag{5}$$

Where $\{T\}$, $\{S\}$, $\{E\}$ are, respectively, the stress, strain and electric potential fields, $\{D\}$ is the electrical displacement field, $[C]$ is the fourth order elasticity tensor, $[\varepsilon]$ are the dielectric constants and $[e]$ the piezoelectric modulus. The superscript T means the transpose of the matrix Expanding the matrices and applying symmetry conditions for 1-3 piezoelectric composites the Eq. (5) can be written as:

$$\begin{Bmatrix} T_{11} \\ T_{22} \\ T_{33} \\ T_{12} \\ T_{23} \\ T_{31} \\ D_1 \\ D_2 \\ D_3 \end{Bmatrix} = \begin{bmatrix} C_{11} & C_{12} & C_{13} & 0 & 0 & 0 & 0 & 0 & e_{13} \\ C_{12} & C_{11} & C_{13} & 0 & 0 & 0 & 0 & 0 & e_{13} \\ C_{13} & C_{13} & C_{33} & 0 & 0 & 0 & 0 & 0 & e_{33} \\ 0 & 0 & 0 & C_{66} & 0 & 0 & 0 & 0 & 0 \\ 0 & 0 & 0 & 0 & C_{44} & 0 & 0 & e_{15} & 0 \\ 0 & 0 & 0 & 0 & 0 & c_{44} & e_{15} & 0 & 0 \\ 0 & 0 & 0 & 0 & 0 & e_{15} & -\varepsilon_{11} & 0 & 0 \\ 0 & 0 & 0 & 0 & e_{15} & 0 & 0 & -\varepsilon_{11} & 0 \\ e_{13} & e_{13} & e_{33} & 0 & 0 & 0 & 0 & 0 & -\varepsilon_{33} \end{bmatrix} \begin{Bmatrix} S_{11} \\ S_{22} \\ S_{33} \\ S_{12} \\ S_{23} \\ S_{31} \\ -E_1 \\ -E_2 \\ -E_3 \end{Bmatrix} \tag{6}$$

Through finite element analysis of the unit cell under prescribed loading cases, average values for stress, strain, electric flux density and electric fields can be evaluated. These average values are used to calculate effective material coefficients according to the following system of equations:

$$\begin{Bmatrix} \{\bar{T}\} \\ \{\bar{D}\} \end{Bmatrix} = \begin{bmatrix} [C]_{eff} & [e]_{eff} \\ [e]_{eff}^{T} & -[\varepsilon]_{eff} \end{bmatrix} \begin{Bmatrix} \{\bar{S}\} \\ -\{\bar{E}\} \end{Bmatrix} \tag{7}$$

Where the upper bar means the average value estimated over the unit cell volume and the subscript *eff* means the effective value. The average values are given by:

$$\bar{T}_{ij} = \frac{1}{V}\int T_{ij}\,dV \tag{8a}$$

$$\bar{S}_{ij} = \frac{1}{V}\int S_{ij}\,dV \tag{8b}$$

$$\bar{D}_{i} = \frac{1}{V}\int D_{i}\,dV \tag{8c}$$

$$\bar{E}_{i} = \frac{1}{V}\int E_{i}\,dV \tag{8d}$$

Where V is the unit cell volume. Using the finite element approach, the average values can be post processed by:

$$\bar{T}_{ij} = \frac{1}{V}\sum_{n=1}^{nel} T_{ij}^{(n)} V^{(n)} \tag{9a}$$

$$\bar{S}_{ij} = \frac{1}{V}\sum_{n=1}^{nel} S_{ij}^{(n)} V^{(n)} \tag{9b}$$

$$\bar{D}_{i} = \frac{1}{V}\sum_{n=1}^{nel} D_{i}^{(n)} V^{(n)} \tag{9c}$$

$$\bar{E}_{i} = \frac{1}{V}\sum_{n=1}^{nel} E_{i}^{(n)} V^{(n)} \tag{9d}$$

Where V is the volume of the unit cell, *nel* is the number of elements modeling the unit cell, $V^{(n)}$ is the volume of the n-th element and $T^{(n)}$, $S^{(n)}$, $D^{(n)}$ and $E^{(n)}$ are the properties evaluated at the n-th element.

3. FINITE ELEMENT MODEL

Several different unit cell configurations have been used according with the loading conditions and fiber arrangement. For the square arrangement, the high symmetry of the model permitted that the same model, showed in fig. 3(a) was used for all loading cases. The hexagonal arrangement uses the model showed in figure 3(b) for cases where displacements normal to the cell faces are imposed or nonzero electric potential just in one face. When shear loading is involved, the RVE must be extended to have complete symmetry between opposite sides (correspondence between opposite nodes) in order to properly apply the constraint equations showed in Eq.(3) and Eq.(4). For shear loading in the x-y plane the model is showed in figure 3(c) and for shear in the y-z plane the model is showed in figure 3(d).

A detailed description of the loading and boundary conditions are presented later, as well as the procedure to obtain the effective material coefficients. All finite element analysis were carried out using the software ANSYS®.

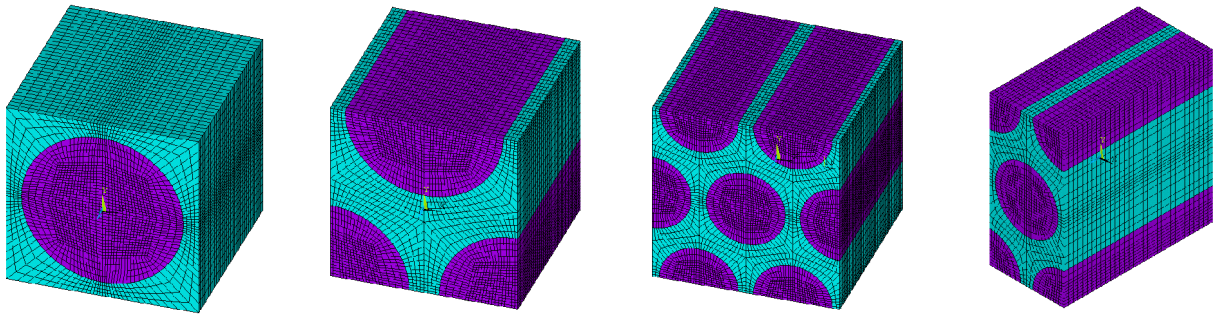

(a) (b) (c) (d)

Figure 3. FE models: (a) square; (b) hexagonal; (c) hexagonal shearing 1-2; (d) hexagonal shearing 2-3

3.1. Material properties

Material properties of both, polymeric matrix and fiber are presented on Table 1. The simulated fiber material is ceramic PZT-5 and the the matrix uses typical polymeric values. Properties of both materials were obtained from Berger *et al.* (2005). For the analysis presented here a fiber volume fraction of 55.5% was adopted.

Table 1. Material Properties for fiber and matrix and composite volume fraction

	C_{11}	C_{12}	C_{13}	C_{33}	C_{44}	C_{66}	e_{13}	e_{15}	e_{33}	ε_{11}	ε_{33}
	x 10^{10} Pa						C / m^2			x 10^{-9} F / m	
Fiber	12.1	7.54	7.52	11.1	2.11	2.28	-5.4	12.3	15.8	8.11	7.35
Matrix	0.386	0.257	0.257	0.386	0.064	0.064	-	-	-	0.0797	0.0797
Fiber volume fraction: 55.5%											

3.2. Analysis procedure

There are several combinations to the order in which the effective coefficients can be calculated. It must be considered first that it is necessary to establish the most reliable results considering the symmetry of the analyzed cell. Most accurate results will be get when the loading is applied in fiber direction, here considered as z-direction. Therefore the first analysis involve the coefficients that can be determined through the application of displacements or electric potential gradients in z-direction.

The prescribed boundary conditions will simplify the set of equations presented in Eq.(6) and it will be possible to evaluate the effective material properties.

1st Analysis: effective C_{13} and C_{33} calculation

Loading and boundary conditions: normal displacements are set as zero on surfaces X+, X-, Y+, Y- and Z-. A positive displacement in Z direction is prescribed on Z+ surface; The electric potential is set to zero on all surfaces. These boundary conditions ensure the compatibility of the unit cell. The zero potential condition leads to $\{E\}=\{0\}$ and the condition for averages $S_{11} = S_{22} = S_{12} = S_{23} = S_{31} = 0$ is ensured by the zero displacement restrictions. As just S_{33} is different of zero, first and third lines from Eq.(6) can be used to obtain C_{13} and C_{33}:

$$C_{13}^{eff} = \bar{T}_{11} / \bar{S}_{33} \tag{10}$$

$$C_{33}^{eff} = \bar{T}_{33} / \bar{S}_{33} \tag{11}$$

2nd Analysis: effective e_{13}, e_{33} and ε_{33} calculation

Loading and boundary conditions: normal displacements are set to zero on all surfaces; Electric potential is set to zero on Z- surface and a prescribed electric potential is applied to the Z+ face. These boundary conditions ensure the compatibility of the unit cell. The zero displacement conditions lead to $\{S\}=\{0\}$ and the applied electrical potential ensures a gradient just in Z direction, so from 1st , 3rd and last lines of Eq.(6), respectively the effective values of e_{13}, e_{33} and ε_{33} can be obtained:

$$e_{13}^{eff} = -\bar{T}_{11} / \bar{E}_{3} \tag{12}$$

$$e_{33}^{eff} = -\bar{T}_{33}/\bar{E}_3 \tag{13}$$

$$\varepsilon_{33}^{eff} = \bar{D}_3/\bar{E}_3 \tag{14}$$

3rd Analysis: effective C_{11} and C_{12} calculation

Loading and boundary conditions: Normal displacements are set as zero X-, Y+, Y-, Z+ and Z- all surfaces; A positive displacement in X direction is prescribed on X+ surface; Electric potential is set to zero on all surfaces. These boundary conditions ensure the compatibility of the unit cell. The zero electric potential condition leads to $\{E\} = \{0\}$ and the condition for averages $S_{22} = S_{33} = S_{12} = S_{23} = S_{31} = 0$ is ensured by the zero displacement restrictions. As just S_{11} is different of zero, first and second lines of Eq. (6) can be used to obtain C_{11} and C_{12}:

$$C_{11}^{eff} = \bar{T}_{11}/\bar{S}_{11} \tag{15}$$

$$C_{12}^{eff} = \bar{T}_{22}/\bar{S}_{11} \tag{16}$$

4th Analysis: effective ε_{11} calculation

Loading and boundary conditions: Normal displacements are set as zero on all surfaces; Electric potential is set to zero on X- surface and a prescribed electric potential is applied to the X+ face. These boundary conditions ensure the compatibility of the unit cell. The zero displacement conditions leads to $\{S\}=\{0\}$ and the applied electrical potential ensures a gradient just in X direction. From the 7th line in Eq. (6):

$$\varepsilon_{11}^{eff} = -\bar{D}_1/\bar{E}_1 \tag{17}$$

5th Analysis: effective C_{66} calculation

Loading and boundary conditions: Z displacements are set as zero on all nodes. All nodes from the center line perpendicular to the X-Y plane have the X and Y displacements set to zero. Two opposite nodes belonging to the fiber border are changed to cylindrical coordinate system and have their angular displacement constrained in order to avoid rigid body rotation. These nodes are in the X-Y plane and make 45° with the coordinate axes. Electric potential is set to zero on all surfaces. Shearing forces of same modulus and opposite orientation are applied on the surfaces Y+ and Y- with X direction and on X+ and X- surfaces with Y direction, producing a pure X-Y shear state. Also the parallelism conditions deduced in Eqs. (3) and (4) must be applied between the pair of surfaces X+ and X-, and between Y+ and Y- surfaces. These boundary conditions ensure the compatibility of the unit cell. As it was forced a pure shear state in X-Y plane, only the component S_{12} from $\{S\}$ is different of zero. The zero electric potential condition ensures that $\{E\}=\{0\}$. Therefore from the 4th line in Eq. (6):

$$C_{66}^{eff} = \bar{T}_{12}/\bar{S}_{12} \tag{18}$$

6th Analysis: effective e_{15} and C_{44} calculation

Loading and boundary conditions: X displacements are set as zero on all nodes. All nodes from the center line perpendicular to the Y-Z plane have the Y and Z displacements set to zero. Two opposite nodes belonging to the center of the fiber in faces Z+ and Z- (Figure 3(d)) are constrained in Y direction in order to avoid rigid body rotation. Electric potential is set to zero on X-, X+, Y- and Y+ surfaces. Shearing forces are applied in the surfaces Y+ and Y- with Z direction, same modulus and opposite orientation and on Z+ and Z- surfaces with Y orientation, producing a pure Y-Z shear state. Also the parallelism conditions deduced in Eqs. (3) and (4) must be applied between the pair of surfaces Z+ and Z-, and between Y+ and Y- surfaces. These boundary conditions ensure the compatibility of the unit cell. Effective ε_{11} was obtained from Eq. (17). Effective values for C_{44} and e_{15} can be obtained from the 5th and 8th lines in Eq. (6):

$$C_{44}^{eff} = (\bar{T}_{23} + \bar{E}_2 e_{15}^{eff})/\bar{S}_{23} \tag{19}$$

$$e_{15}^{eff} = (-\bar{E}_2 \varepsilon_{11} + \bar{D}_2)/\bar{S}_{23} \tag{20}$$

4. RESULTS

According to the procedure discussed above, the obtained results for the properties involved in the effective coefficients calculation are presented in Figures 3. and 4. for fibers with square and hexagonal arrangement, respectively. The average values are calculated from the finite element results through the set of Eqs. (9a) to (9d). Standard finite elements calculations already uses and calculates element average values, as well as individual element

volumes, so these equations can easily be post-processed in a commercial finite element code. Eqs. (10) to (20) are used to obtain the effective coefficients.

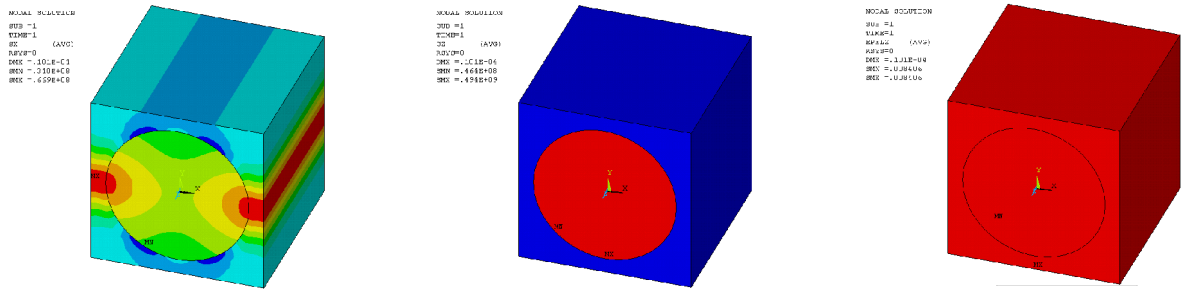

(a) First analysis: respectively T_{11}, T_{33}, and S_{33}

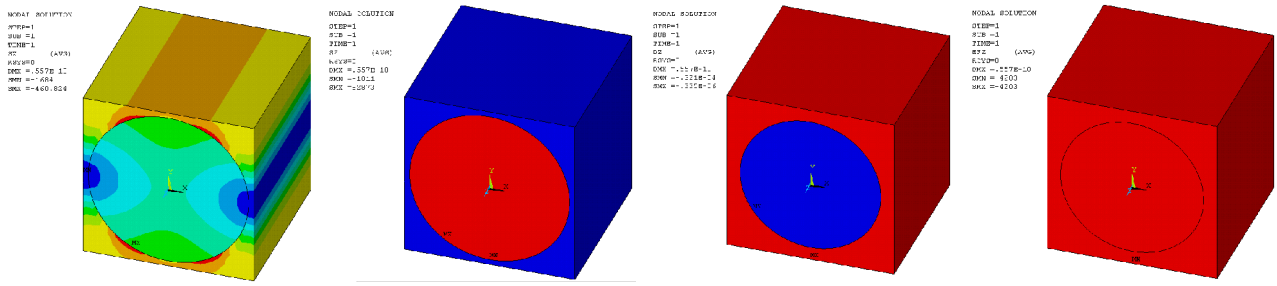

(b) Second analysis: T_{11}, T_{33}, D_3 and E_3

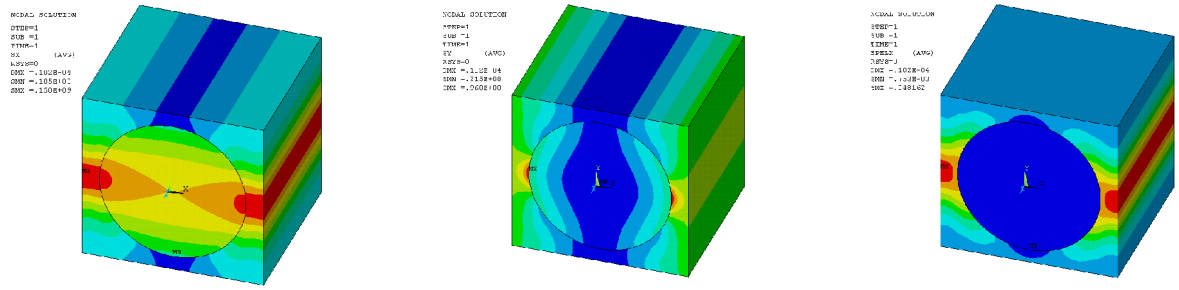

(c) Third analysis: T_{11}, T_{22} and S_{11}

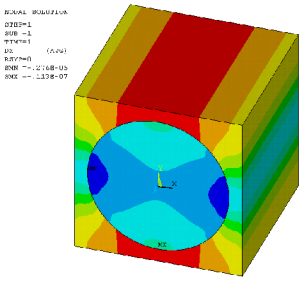

(d) Fourth analysis: D_1 and E_1

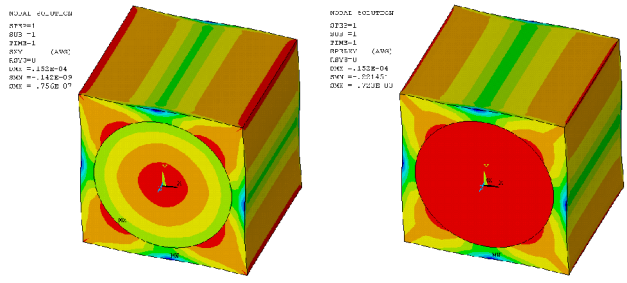

(e) Fifth analysis: T_{12} and S_{12}

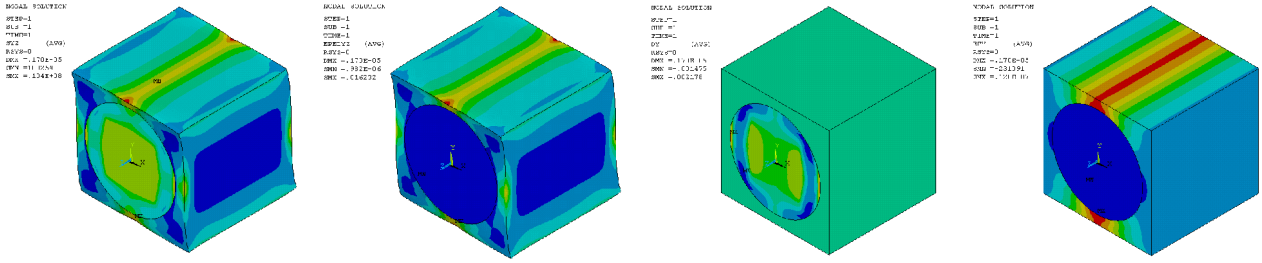

(f) Sixth analysis: T_{23}, S_{23}, D_2 and E_2

Figure 4. Square arrangement: non-zero average fields for each analysis

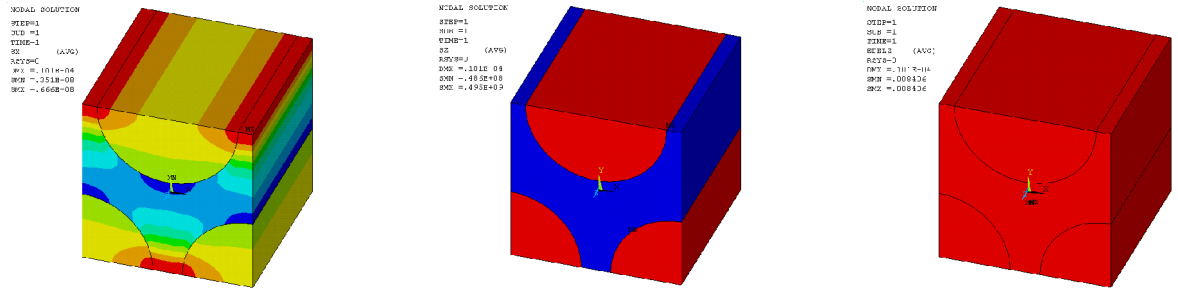

(a) First analysis: T_{11}, T_{33} and S_{33}

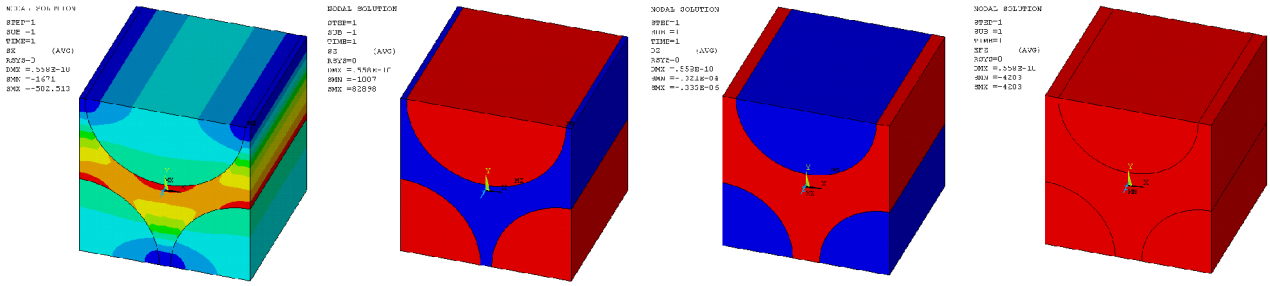

(b) Second analysis: T_{11}, T_{33}, D_3 and E_3

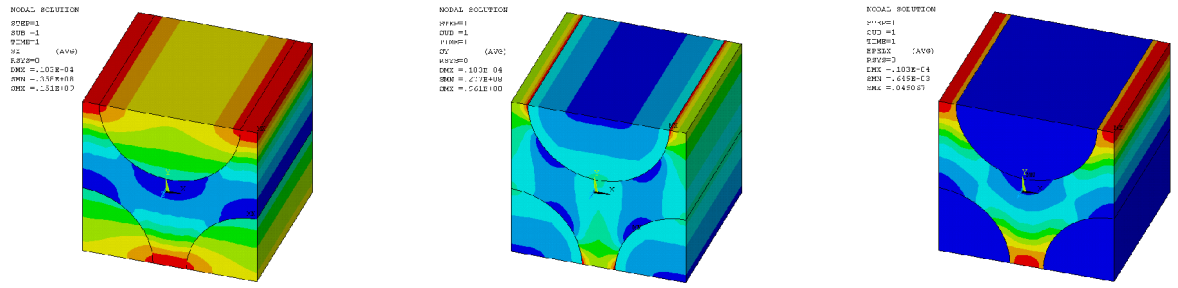

(c) Third analysis: T_{11}, T_{22}, S_{11}

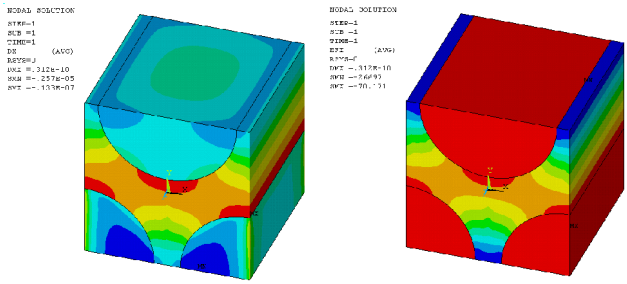

(d) Fourth analysis: D_1 and E_1

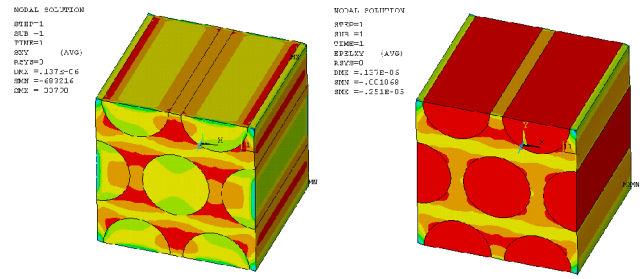

(e) Fifth analysis: T_{12} and S_{12}

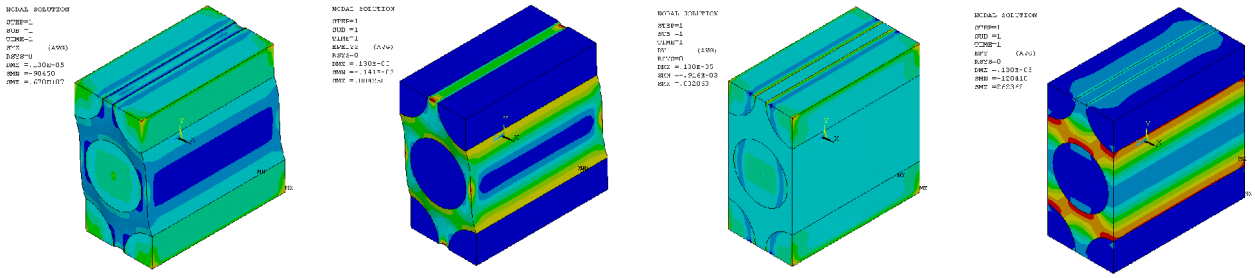

(f) Sixth analysis: T_{23}, S_{23}, D_2 and E_2

Figure 5. Hexagonal arrangement: non-zero average fields for each analysis

All the results are summarized in the Table 2, where, the columns designed as (1) and (2) refers to the results obtained by Berger *et al.* (2005), estimated from graphs presented in their paper. (1) refers to analytical results obtained

by asymptotic homogenization and (2) numerical results obtained by finite element analysis. The columns designed by (3) and (4) summarize the coefficients obtained by the analysis procedure presented in this work. They refer respectively to square fiber arrangement and hexagonal arrangement The values obtained to the effective coefficients are compared using analytical results as reference, and the estimated error is presented in the three last columns of Table 2, where the first column of errors is taken between the analytical and numerical results presented by Berger *et al.* (2005), the second between analytical and square arrangement and the third between analytical and hexagonal arrangement..

Table 2. Analytical and numerical results comparison

Coefficient	Units	(1)	(2)	(3)	(4)	Error [%][(a)]	Error [%][(b)]	Error [%][(c)]
C_{11}	x 10^{10} Pa	0.95	1.10	1.088	1.068	15.8	14.5	12.4
C_{12}		0.56	0.48	0.465	0.522	14.3	17.1	6.8
C_{13}		0.60	0.60	0.604	0.619	0.0	0.7	3.2
C_{33}		3.50	3.50	3.525	3.521	0.0	0.7	0.6
C_{44}		0.22	0.18	0.215	0.195	18.2	2.3	11.4
C_{66}		0.20	0.16	0.154	0.181	20.0	23.1	9.5
e_{13}	C / m^2	-0.26	-0.26	-0.258	-0.269	0.0	0.7	3.5
e_{15}		0.02	0.018	0.0241	0.0164	10.0	20.5	18.0
e_{33}		11.0	11.0	10.86	10.86	0.0	1.3	1.3
ε_{11}	x 10^{-9} F/m	0.28	0.29	0.284	0.303	3.6	1.4	8.2
ε_{33}		4.20	4.20	4.27	4.27	0.0	1.6	1.6

(1) BERGER *et al.* (2005) analytical results (estimated from graphs);
(2) BERGER *et al*. (2005) numerical results with square fiber arrangement (estimated from graphs);
(3) Numerical results presented in this report – square fiber arrangement;
(4) Numerical results presented in this report – hexagonal fiber arrangement.

[(a)] : Comparing (1) and (2);
[(b)] : Comparing (1) and (3);
[(c)] : Comparing (1) and (4).

5. CONCLUSIONS

The presented models had, in general, a good agreement with analytical results obtained by the asymptotic homogenization. Numerical results presented here are very similar to results reported by Berger *et al.* for the square arrangement of fibers. The applied boundary conditions and procedure analysis have been considered suitable for analyzing 1-3 piezoelectric composites. Adopting the same procedures, models to represent hexagonal fiber arrangement are presented. Using this finite element model, the estimated errors between numerical and analytical results are reduced to less than 12.5% except for the e_{15} coefficient. This coefficient is strongly dependent on S_{23} strains, so also strongly dependent on boundary conditions applied to reproduce the symmetric behavior of the unit cell. The general improvement on quality of results using the hexagonal arrangement instead the square is expected because the transverse isotropy hypothesis is fulfilled, which is not the case for square arrangement. It is important to mention that the authors have carried out new investigations which will be submitted to publish in the future.

6. REFERENCES

Azzouz, M.S., Mei, C., Bevan, J.S. and Ro, J.J., 2001, "Finite element modeling of MFC/AFC actuators and performance of MFC", Journal of Intelligent Material Systems and Structures, vol.12, pp.601-612.

Berger, H., Kari, S., Gabbert, U., Rodriguez-Ramos, R., Guinovart, R., Otero, J.A. and Bravo-Castillero, J., 2005, "An analytical and numerical approach for calculating effective material coefficients of piezoelectric fiber composites", International Journal of Solids and Structures, vol. 42, pp. 5692-5714.

Bisegna, P. and Luciano, R., 1996, "Variational bounds for the overall properties of piezoelectric composites", Journal of the Mechanics and Physics of Solids, vol.44, pp.583-602.

Bisegna, P. and Luciano, R., 1997, "On methosds for bounding the overall properties of periodic piezoelectric fibrous composites", Journal of the Mechanics and Physics of Solids, vol.45, pp.1329-1356.

Bravo-Castillero, J., Guinovart-Diaz, R., Sabina, F.J. and Rodríguez-Ramos, R., 2001, "Closed form expressions for the effective coefficients of a fiber-reinforced composite with transversely isotropic constituents – II. Piezoelectric and square symmetry", Mechanics of Materials, vol.33, pp.237-248.

Chan, H.L.W. and Unsworth, J., 1989, "Simple model for piezoelectric ceramic/polymer 1-3 composites used in ultrasonic transducer applications", IEEE Transactions on Ultrasonics, Ferroelectrics and Frequency Control, vol.36, pp.434-441.

Dent, A.C., Nelson, L.J., Bowen, C.R., Stevens, R., Cain, M. and Stewart, M., 2005, "Characterization and properties os fine scale PZT fibres", Journal of the European Ceramic Society, vol.25, pp.2387-2391.

Dunn, M.L. and Taya, M., 1993, "Micromechanics predictions of the effective electroelastic moduli of piezoelectric composites", International Journal of Solids and Structures, vol.30, pp.161-175.

Gaudenzi, P., 1997, "On the electo mechanical response of active composite materials with piezoelectric inclusions", Computers & Structures, vol.65, pp.157-168.

Guinovart-Díaz, R., Bravo-Castillero, J., Rodríguez-Ramos, R., Sabina, F.J. and Martínez-Rosado, R., 2001, "Overall properties of piezocomposite materials 1-3", Materials Letters, vol.48, pp.93-98.

Guinovart-Díaz, R., Bravo-Castillero, J., Rodríguez-Ramos, R., Martínez-Rosado, R., Serranía, F. and Navarrete, M., 2002, "Modeling of elastic transversely isotropic composite using the asymptotic homogenization method. Some comparisons with other models", Materials Letters, vol.56, pp.889-894.

Kar-Gupta, R. and Venkatesh, T.A., 2005, "Electromechanical response of 1-3 piezoelectric composites: effect of poling characteristics", Journal af Applied Physics, vol.98, 14p.

Kar-Gupta, R. and Venkatesh, T.A., 2007a, "Electromechanical response of 1-3 piezoelectric composites: an analytical model", Acta Materialia, vol.55, pp.1093-1108.

Kar-Gupta, R. and Venkatesh, T.A., 2007b, "Electromechanical response of 1-3 piezoelectric composites: a numerical model to assess the effects of fiber distribution", Acta Materialia, vol.55, pp.1275-1292.

Melnykowycz, M., Kornmann, X., Huber, C., Barbezat, M. and Brunner, A.J., 2006, "Performance of integrated active fiber composites in fiber reinforced epoxy laminates", Smart Materials and Structures, vol.15, pp.204-212.

Paik, S.H., Yoon, T.H., Shin, S.J. and Kim, S.J., 2007, "Computational material characterization of active fiber composite", Journal of Intelligent Material Systems and Structures, vol.18, pp.19-28.

Panda, S. and Ray, M.C., 2006, "Nonlinear analysis of smart functinally graded plates integrated with a layer of piezoelectric fiber reinforced composite", Smart Materials and Structures, vol.15, pp.1595-1604.

Panda, S. and Ray, M.C., 2008, "Nonlinear finite element analysis of functionally graded plates integrated with patches of piezoelectric fiber reinforced composite", Finite Elements in Analysis and Design, vol.44, pp.493-504.

Paradies, R. and Melnykowycz, M., 2007, "Numerical stress investigation for piezoelectric elements with circular cross section and interdigitated electrodes", Journal of Intelligent Material Systems and Structures, vol.18, pp.963-972.

Pettermann, H.E. and Suresh, S., 2000, "A comprehensive unit cell model: a study of coupled effects in piezoelectric 1-3 composites", International Journal of Solids and Structures, vol.37, pp.5447-5464.

Poizat, C. and Sester, M., 1999, "Effective properties of composites with embedded piezoelectric fibres", Computational Materials Science, vol.16, pp.89-97.

Rodríguez-Ramos, R., Sabina, F.J., Guinovart-Díaz, R. and Bravo-Castillero, J., 2001, "Closed form expressions for the effective coefficients of a fiber-reinforced composite with transversely isotropic constituents – I. Elastic and square symmetry", Mechanics of Materials, vol.33, pp.223-235.

Sevostianov, I., Levin, V. and Kachanov, M., 2001, "On the modeling and design of piezocomposites with prescribed properties", Archive of Applied Mechanics, vol.71, pp.733-747.

Smith, W.A. and Auld, B.A., 1991, "Modeling 1-3 composite-piezoelectrics: thickness-mode oscillations", IEEE Transactions on Ultrasonics, Ferroelectrics and Frequency Control, vol.38, pp.40-47.

Tan, X.G. and Vu-Quoc, L., 2005, "Optimal solid shell element for large deformable composite structures with piezoelectric layers and active vibration control", International Journal for Numerical Methods in Engineering, vol.64, pp.1981-2013.

7. RESPONSIBILITY NOTICE

The authors are the only responsible for the material included in this paper.